

CrossMark  
click for updatesCite this: *J. Mater. Chem. A*, 2014, 2, 12686Received 3rd May 2014  
Accepted 16th June 2014

DOI: 10.1039/c4ta02214a

www.rsc.org/MaterialsA

## A nickel-modified polyoxometalate towards a highly efficient catalyst for selective oxidation of hydrocarbons†

Lei Zhou, Juan Liu, Wenbin Ji, Hui Huang, Hailiang Hu, Yang Liu\* and Zhenhui Kang\*

A nickel-modified polyoxometalate compound was synthesized which exhibited excellent catalytic activity (conversion: 41.63%; selectivity: 97.21%) for selective oxidation of cyclooctene using air as an oxidant without a solvent.

Polyoxometalates (POMs) exhibit a great diversity of sizes, nuclearities, and shapes with diverse physical properties and applications, such as catalysis,<sup>1–6</sup> electrochemistry,<sup>7,8</sup> medicine,<sup>9</sup> and so on.<sup>10–12</sup> Especially, the interest in catalysis by POM-based coordination polymers has significantly grown because the structures of the catalytically active sites can be designed at atomic and molecular levels.<sup>13–16</sup> The design and synthesis of POM-based coordination polymers with specific catalytic properties are the core issues of the current catalysis chemistry and still remain to be actively explored.<sup>17–19</sup>

Oxidation is an important pathway for large-scale production of chemicals. Hydrocarbon selective oxidation has attracted much attention because the related products of epoxides are valuable and resourceful commercial intermediates for many end products such as pharmaceuticals, fine chemicals, polycarbonates, ethers and glycols.<sup>20–22</sup> However, poor efficiency of selective oxidation of hydrocarbons is the common drawback. Recently, the important concept of “green chemistry” has been associated with this type of catalytic reaction, which involves the use of molecular oxygen directly from air.<sup>23–27</sup> The design of highly effective catalysts with high yields and selectivities is a challenging task for oxidation reactions, especially hydrocarbon oxidation reactions, using air as an oxidant.

The catalytic function of POMs in the oxidation of alkene has been extensively reviewed.<sup>28–34</sup> Various catalytic systems for H<sub>2</sub>O<sub>2</sub>-based epoxidation catalyzed by POMs have been developed.<sup>35,36</sup> For example, Xi Zuwei's group reported a tungsten-containing catalyst for the epoxidation of olefins. When catalytic epoxidation of propylene was performed at 65 °C with H<sub>2</sub>O<sub>2</sub>, the conversion was 85% and the selectivity was 95%.<sup>37</sup> However, in most cases, the use of an excess amount of hydrogen peroxide and low pH in an aqueous phase in the case of the biphasic systems leads to the low efficiency of hydrogen peroxide utilization and selectivity for epoxides.

Transition-metal compounds such as metalloporphyrin, manganese complexes and tungsten compounds have been used as effective catalysts for homogeneous and heterogeneous epoxidation with hydrogen peroxide.<sup>38–41</sup> Especially, nickel catalysts play an important role in catalytic processes.<sup>42</sup> Although a few investigations have been focused on nickel compounds as alkene oxidation catalysts, most of these studies are limited to the use of NaClO, PhIO, *t*-BuOOH and H<sub>2</sub>O<sub>2</sub> as terminal oxidants.<sup>43,44</sup> These epoxidation processes using above various catalysts and oxidants have disadvantages from the economical viewpoint because they are very capital intensive.

Indeed, integration of different functional units into one hybrid system may give birth to desired materials. In such a way, combining two species, such new nickel-modified POMs could function as potential new synergy catalysts in a cooperative catalysis fashion, and then reinforce their catalytic abilities. Relevant research about the catalytic performance of a hybrid complex Ni(salen)–POM (salen = *N,N'*-bis(salicylidene)ethylenediamine) in the epoxidation of olefins has been reported.<sup>45</sup> Using hydrogen peroxide as an oxygen source, higher yields can be obtained in the epoxidation of various olefins in acetonitrile. But the epoxide selectivity was not satisfactory and the oxidant involved high cost.

Undoubtedly, to promote green chemistry and atom efficiency, the use of large amounts of volatile organic solvents and activators should be avoided. Furthermore, use of inexpensive and environmentally friendly oxidants like oxygen from air

*Institute of Functional Nano & Soft Materials (FUNSOM) and Collaborative Innovation Center of Suzhou Nano Science and Technology, Soochow University, Suzhou 215123, China. E-mail: zhkang@suda.edu.cn; yangl@suda.edu.cn; Fax: +86-512-65882846; Tel: +86-512-65880957*

† Electronic supplementary information (ESI) available: Detailed experimental section, figures, IR spectra, TG curves, together with tables. CCDC 997868. For ESI and crystallographic data in CIF or other electronic format see DOI: 10.1039/c4ta02214a

must be an intriguing task, which greatly overcomes the disadvantages of all the above terminal oxidants. Recently, we tried to synthesize a POM-based hybrid with a covalently linked Fsa ligand (a widely used antifungal medicine as well as a good flexible nitrogenous ligand). Herein, a new POM-based hybrid compound with a three-dimensional (3D) framework,  $[\text{Ni}_2(\text{Fsa})_7(\text{H}_2\text{O})(\text{SiMo}_{12}\text{O}_{40})] \cdot \text{H}_2\text{O}$  (**1**), has been fabricated under hydrothermal conditions. We demonstrated that **1** can be used as an excellent catalyst for the selective oxidation of cyclooctene, which shows 41.63% conversion based on cyclooctene and 97.21% selectivity for epoxycyclooctane with *tert*-butyl hydroperoxide (TBHP) as an initiator at 80 °C. It is worth mentioning that the oxidant is air, which shows that the selective oxidation of cyclooctene proceeds under mild conditions that can be energy-saving, environmentally friendly, and low cost.

In our experiments, compound **1** was prepared through a hydrothermal method by using a mixture of  $\text{Na}_2\text{SiO}_3 \cdot 2\text{H}_2\text{O}$ ,  $\text{Na}_2\text{MoO}_4$ ,  $\text{Ni}(\text{Ac})_2$ , Fsa and distilled water at 150 °C for 3 days. Crystal structure analysis reveals that compound **1** is composed of one Keggin-type  $[\text{SiMo}_{12}\text{O}_{40}]^{4-}$  anion (abbreviated as  $\text{SiMo}_{12}$ ), three Ni ions, seven Fsa ligands, one lattice and one coordinated water molecules (Fig. 1a). Bond valence sum calculations show that the Ni and Mo atoms are in +2 and +6 oxidation states, respectively.<sup>46</sup> In **1**, the three independent Ni ions (Ni1, Ni2 and Ni3) exhibit similar octahedral coordination geometries (Fig. S1†). Ni1 and Ni2 are six-coordinated by four N atoms from four Fsa ligands and two terminal O atoms ( $\text{O}_t$ ) from two  $\text{SiMo}_{12}$  anions. Ni3 is coordinated by two N atoms from two Fsa ligands, two  $\text{O}_t$  atoms and two coordinated water molecules. All

the bond distances around the Ni centers are normal (Table S2†). The local coordination geometry around Ni atoms in **1** can be regarded as an octahedron (4 + 2 coordination modes of  $\text{NiN}_2\text{O}_4$  and  $\text{NiN}_4\text{O}_2$  moieties). The  $\text{SiMo}_{12}$  clusters act as tetradentate inorganic ligands with their four  $\text{O}_t$  atoms being coordinated to four Ni centres. Through the bridge of metal complex units, each  $\text{SiMo}_{12}$  anion connects with four adjacent  $\text{SiMo}_{12}$  clusters, forming a diamond-like network (Fig. 1b). Extension of the diamond net gives birth to a 3D framework of **1**. Further structural analysis reveals that two coordination sites of the Ni3 sphere are occupied by water molecules (Fig. 1c). In contrast to the Fsa ligand, the coordinated water molecules could be easily removed in a vacuum or at elevated temperature to leave open Ni active sites, which would exhibit excellent catalytic activity in catalysis. Topological analysis of the framework has been performed by considering each  $\text{SiMo}_{12}$  anion as a 4-connected node and each Ni complex unit as a linker. Thus the whole structure of **1** can be characterized as a 4-connected 3D network with a  $6^6$  topology (Fig. S2†).

To investigate the thermal stability of **1**, a thermogravimetric (TG) study was carried out under a  $\text{N}_2$  atmosphere with a heating rate of 10 °C  $\text{min}^{-1}$  in the temperature range of 22 to 1000 °C (Fig. S3†). The weight loss of about 0.62% from 25 to 51 °C is consistent with the loss of water molecules (calcd 0.86%), while the total weight loss of 47.44% from 160 to 620 °C arises from the decomposition of the Fsa ligand. Powder X-ray diffraction (XRPD) of **1** has been measured to confirm the phase purity and to examine the crystallinity of bulk samples (Fig. 4b). The differences in intensity may be due to the preferred orientation of the crystalline powder sample.

To study the redox properties of **1**, the compound **1** bulk-modified carbon paste electrode (CPE) was fabricated as the working electrode owing to the insolubility of the POM-based inorganic–organic hybrids prepared by hydrothermal reaction in water and poor solubility in common organic solvents. The cyclic voltammetry of compound **1** was performed in a 1 mol  $\text{L}^{-1}$   $\text{H}_2\text{SO}_4$  aqueous solution. As shown in Fig. 2a, there are three reversible redox peaks in the potential range of 600 to –100 mV. Redox peaks I–I', II–II' and III–III' correspond to reduction and oxidation of  $\text{SiMo}_{12}$  anions through three consecutive two-electron processes respectively,<sup>47–50</sup> which suggests that the  $\text{SiMo}_{12}$  anions are the active centres for redox behaviors. With the increase of the scan rates, the cathodic peak potentials shift

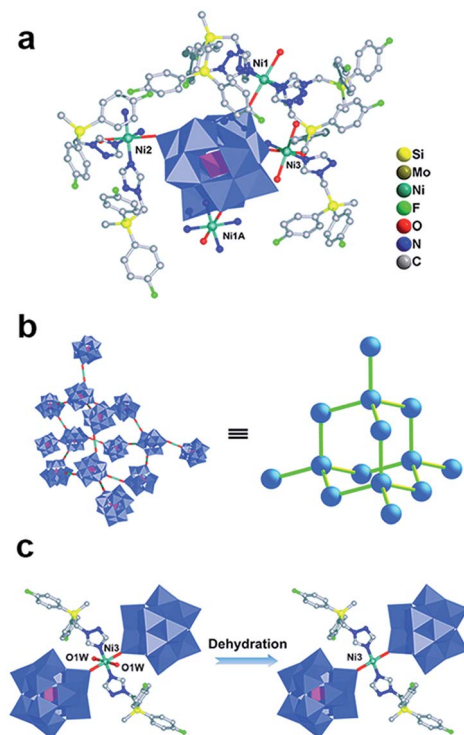


Fig. 1 (a) Stick/polyhedral view of the asymmetric unit of **1**. (b) Diamond-like construction. (c) The dehydration process of Ni3.

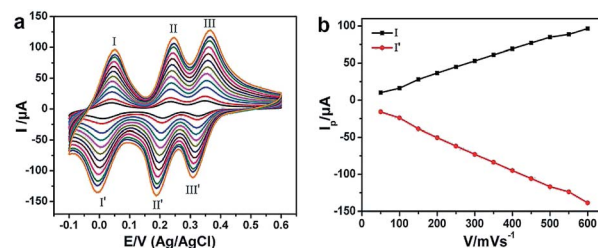


Fig. 2 (a) Cyclic voltammograms of **1**–CPE in a 1 M  $\text{H}_2\text{SO}_4$  solution at different scan rates (from inner to outer: 50, 100, 150, 200, 250, 300, 350, 400, 450, 500, 550 and 600  $\text{mV s}^{-1}$ ). (b) The dependence of anodic peak (I) and cathodic peak (I') current of **1**–CPE on scan rates.

to the negative direction and the corresponding anodic peak potentials shift to the positive direction (Fig. 2b). The peak currents are proportional to the scan rates, indicating that the redox process of 1-CPE is surface-controlled.

In the following experiments, the catalytic activity of **1** (size of particles about 5  $\mu\text{m}$ , see the scanning electron microscopy (SEM) image in Fig. S5†) was investigated for oxidation of cyclooctene in the absence of solvents using TBHP as a radical initiator and oxygen (in air) as an oxidant at 80 °C. The oxidation products were analyzed by gas chromatography (GC) and gas chromatography-mass spectroscopy (GC-MS). The detailed conversion of cyclooctene and selectivity for oxidation products are shown in Table S3.† Fig. 3a demonstrates that a high conversion of cyclooctene and selectivity for epoxycyclooctane were achieved simultaneously after 48 h. The conversion of cyclooctene increased from 23.81 to 41.63% after 48 h. The selectivity for epoxycyclooctane also increased from 84.53 up to 97.21%. However, the selectivity for 2-cyclooctenone decreased from 15.47% to 1.61% with increasing reaction time. The total selectivity for epoxycyclooctane and 2-cyclooctenone shown in Table S3† is less than 100% (98.85%), which ascribes to a part of  $\text{C}_8$  oxidation products that might further be oxidized to other carbon oxides, such as carbon dioxide that would not be measured under present conditions.<sup>51,52</sup> In the control experiments, the catalytic performance of  $\text{Ni}(\text{Ac})_2$  and  $\text{SiMo}_{12}$  in the selective oxidation of cyclooctene was further studied under the same conditions to confirm the catalytic activity of compound **1**, and the detailed results are shown in Fig. 3b and Table S4.† Among the three materials, compound **1** yielded the highest catalytic activity. In contrast, the  $\text{Ni}(\text{Ac})_2$  and  $\text{SiMo}_{12}$  species show the relatively low conversion to cyclooctene. These results

indicate that there is a synergy between Ni-Fsa complex units and  $\text{SiMo}_{12}$  anions. All the above results prove that compound **1** indeed exhibits high catalytic activity. The scope of the present catalytic system was examined. This catalytic system can also be applied to oxidation of other olefins (such as cyclohexene, 1-octene and  $\alpha$ -methylstyrene) in air. Excellent catalytic activity (conversion: 46.02% to cyclohexene, 38.23% to 1-octene and 39.75% to  $\alpha$ -methylstyrene; selectivity: 92.34% for epoxy-cyclohexene, 98.56% for 1,2-epoxyoctane and 93.71% to acetophenone, respectively) was also observed in the oxidation of such olefins.

In order to demonstrate that compound **1** is stable enough for catalytic cycles. The catalyst (compound **1**) was separated from the reaction solution after the first catalytic run, washed several times with dichloromethane to remove the physisorbed molecules, dried and reused in another catalytic cycle. A series of catalytic experiments suggested that, as a catalyst, compound **1** still retained its catalytic activity (with nearly constant conversion and selectivity, see Fig. 3c) and was stable (XRPD, see Fig. 3d) after five catalytic cycles. The catalytic cycle results are similar to those of the first catalytic run. The composition of the product changed with increasing reaction time. The selectivity for epoxycyclooctane increased up to about 97.21% and the selectivity for 2-cyclooctenone decreased with increasing reaction time during the catalytic cycles. Further blank reactions (*i.e.*, without catalyst) did not result in any epoxide and/or other products being produced. Furthermore, the filtrate solution test (additional 48 h reaction after removing the compound **1** from the reaction medium) showed no catalytic activity, which indicated that the catalytic activity of compound **1** originated from the presence of the solid catalyst and was not caused by molecular species that dissolved into solution. All the above-mentioned catalytic experiments show that compound **1** indeed acts as a heterogeneous catalyst in the present catalytic system.

For further confirming the point that synergy between Ni-Fsa complex units and  $\text{SiMo}_{12}$  anions results in active sites during the catalytic oxidation process, several control experiments were carried out to investigate the active sites in the catalytic oxidation process. The catalytic performance of compound **1** with dehydration treatment and non-dehydration treatment was further studied at 30 °C for the selective oxidation of cyclooctene. The catalytic performances in Table 1 show

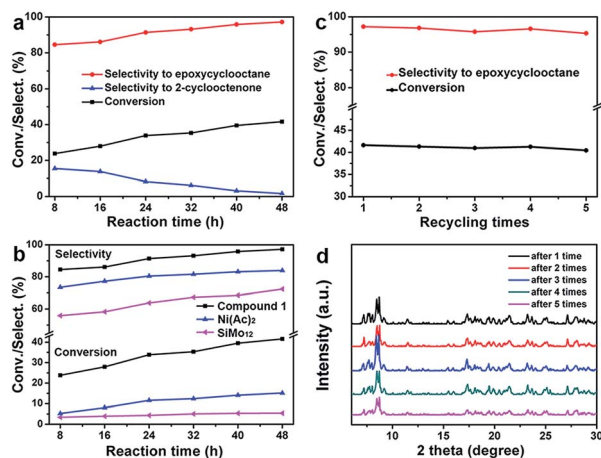
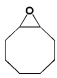
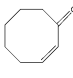


Fig. 3 (a) The relationship between the conversion of cyclooctene/selectivity to different products and reaction time with compound **1** as a catalyst; (b) the relationship between the conversion of cyclooctene/selectivity to epoxycyclooctane and reaction time with compound **1** (black line),  $\text{Ni}(\text{Ac})_2$  (blue line) and  $\text{SiMo}_{12}$  (pink line) as catalysts, respectively. (c) The relationship between the conversion of cyclooctene/selectivity of epoxycyclooctane and recycling times with compound **1** as a catalyst five times. (d) The XRPD patterns based on the single-crystal structure of **1**: after 1 (black line), 2 (red line), 3 (blue line), 4 (green line), and 5 (pink line) times recycling.

Table 1 The effect of compound **1** with dehydration and non-dehydration treatment as catalysts on selective oxidation of cyclooctene<sup>a</sup>

Catalyst	Product selectivity (%)		Conversion (%)	$\Sigma_{\text{sel}}\text{C}_8^b$
				
Dehydration	96.72	2.07	14.13	98.79
Non-dehydration	96.45	2.28	6.34	98.73

<sup>a</sup> Reaction conditions: compound **1** (200 mg), cyclooctene (10 mL), TBHP (0.12 g), 30 °C. <sup>b</sup> Total selectivity for  $\text{C}_8$  partial oxidation products.

that compound **1** with dehydration treatment still exhibits good catalytic activity for the oxidation of cyclooctene with a conversion of 14.13% and a selectivity of 96.72% for epoxy-cyclooctane in 48 h, which are clearly superior to those of compound **1** with non-dehydration treatment (merely a conversion of 6.34% and a selectivity of 96.45% for epoxy-cyclooctane in 48 h). The reactive species trapping experiments were carried out with two different scavengers, *tert*-butanol (a HO<sup>•</sup> radical scavenger) and benzquinamide (BZQ, an O<sup>2•−</sup> radical scavenger) to check the active oxygen species generated in the present catalytic system. Fig. S6† shows the catalytic results after addition of two different scavengers. The addition of *tert*-butanol substantially reduced the catalytic activity for the oxidation of cyclooctene from almost 41.63% to 3.53% after 48 h reaction, while the introduction of BZQ barely affects the catalytic activity. All of the above experiments confirm that HO<sup>•</sup> is the active oxygen species in this catalytic oxidation process.

A further detailed analysis of the TG and differential thermal gravity (DTG) curves (in the range of 22 to 100 °C, Fig. 4a) indicates that the water molecules begin to be removed at 25 °C, as the weight loss of free water molecules begins at that temperature. With increasing temperature, the coordinated water molecules are gradually lost. When the temperature reaches about 51 °C, the water molecules are lost completely. The dehydration treatment of **1** with respect to temperature has been also monitored by temperature-dependent XRPD as shown in Fig. 4b. Compound **1** was heated at 100 °C for dehydration treatment, and then XRPD analysis was carried out on the dehydration sample. The phase purity is in good match between the XRPD pattern of the dehydration sample and the simulated pattern. Furthermore, a series of evacuated peaks (the 2θ values range from 10 to 18) show that there is a slight framework distortion with dehydration treatment.<sup>53</sup> Combining the XRPD pattern, TG and DTG curves, we conclude that active sites can be generated at a certain temperature (above 51 °C) because of removal of coordinated water molecules around the Ni3 atom. The above results demonstrate that the excellent catalytic

activity of compound **1** is indeed ascribed to the active sites resulting from synergy between Ni-Fsa complex units and SiMo<sub>12</sub> anions.

On the basis of these results and discussion below, we propose a possible reaction mechanism for this catalytic reaction as shown in Fig. 4c. The octahedral coordination sphere around the Ni3 atom is completed with water molecules, Fsa ligands and SiMo<sub>12</sub> anions. In contrast to Fsa and SiMo<sub>12</sub> species, the coordinated water molecules are easily removed at elevated temperature.<sup>54–58</sup> The dehydration makes the nickel coordination sites accessible for other molecules, which facilitates oxygen molecules accessible to the nickel centre.<sup>59–61</sup> What is more, the Mo=O group in SiMo<sub>12</sub> further results in an activation of the oxygen molecules due to the excellent redox properties of POMs. In addition, TBHP acts as a free radical initiator with oxygen in air as the oxidant, while the C=C bond is directly oxidized by the active oxygen radicals generated from the radical initiator and oxygen.<sup>62</sup> As a consequence, the combination of both SiMo<sub>12</sub> and Ni-Fsa complex units in a cooperative catalysis fashion results in a reasonable conversion of 41.63% after 48 h and a high selectivity for oxidation of cyclooctene. Here we also need to further point out that the present catalyst system is endowed with the structure tunable ability, and then its catalytic abilities may further be improved by using different POMs ([SiW<sub>12</sub>O<sub>40</sub>]<sup>4−</sup>, [PW<sub>12</sub>O<sub>40</sub>]<sup>3−</sup>, etc.), organic ligands (1,10-phenanthroline monohydrate, 2,2′-bipyridine, etc.) and metals (Co, Cu, Ag, etc.).

In summary, we have prepared a new POM-based hybrid compound combined with nickel and the Fsa ligand, which exhibits excellent catalytic activity for oxidation of cyclooctene. The significance of **1** not only extends the design and synthesis of the POM-based hybrid family as multifunctional materials but also provides new promising materials as catalysts in the hydrocarbon selective oxidation field. It is believed that more POM-based coordination polymers with interesting structures and specific catalytic properties will be synthesized in future.

## Acknowledgements

This work was supported by the National Basic Research Program of China (973Program) (2012CB825800 and 2013CB932702), the National Natural Science Foundation of China (51132006), the Specialized Research Fund for the Doctoral Program of Higher Education (20123201110018), a Suzhou Planning Project of Science and Technology (ZXG2012028), and a project funded by the Priority Academic Program Development of Jiangsu Higher Education Institutions.

## Notes and references

- 1 A. Dolbecq, E. Dumas, C. R. Mayer and P. Mialane, *Chem. Rev.*, 2010, **110**, 6009–6048.
- 2 I. V. Kozhevnikov, *Chem. Rev.*, 1998, **98**, 171–198.
- 3 T. Hirano, K. Uehara, K. Kamata and N. Mizuno, *J. Am. Chem. Soc.*, 2012, **134**, 6425–6433.

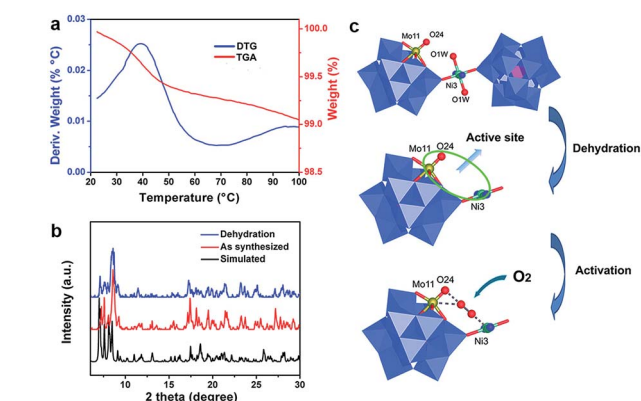


Fig. 4 (a) Partial TG and DTG curves of the compound **1** measured from 22 °C to 100 °C under a N<sub>2</sub> atmosphere. (b) XRPD spectra of compound **1**. Dehydrated one (blue line), as-synthesized one (red line), and simulated one (dark line). (c) Schematic illustration of the proposed mechanism for activation of the oxygen molecule.

- 4 E. Derat, D. Kumar, R. Neumann and S. Shaik, *Inorg. Chem.*, 2006, **45**, 8655–8663.
- 5 N. V. Maksimchuk, K. A. Kovalenko, S. S. Arzumanov, Y. A. Chesalov, M. S. Melgunov, A. G. Stepanov, V. P. Fedin and O. A. Kholdeeva, *Inorg. Chem.*, 2010, **49**, 2920–2930.
- 6 Q. X. Han, C. He, M. Zhao, B. Qi, J. Y. Niu and C. Y. Duan, *J. Am. Chem. Soc.*, 2013, **135**, 10186–10189.
- 7 M. Sadakane and E. Steckhan, *Chem. Rev.*, 1998, **98**, 219–238.
- 8 C. Debiemme-Chouvy and H. Cachet, *J. Phys. Chem. C*, 2008, **112**, 18183–18188.
- 9 J. T. Rhule, C. L. Hill, D. A. Judd and R. F. Schinazi, *Chem. Rev.*, 1998, **98**, 327–358.
- 10 T. R  ther, V. M. Hultgren, B. P. Timko, A. M. Bond, W. R. Jackson and A. G. Wedd, *J. Am. Chem. Soc.*, 2003, **125**, 10133–10143.
- 11 T. Yamase and P. V. Prokop, *Angew. Chem., Int. Ed.*, 2002, **41**, 466–469.
- 12 P. Mialane, C. Duboc, J. Marrot, E. Riviere, A. Dolbecq and F. S  cheresse, *Chem.–Eur. J.*, 2006, **12**, 1950–1959.
- 13 N. Mizuno, S. Hikichi, K. Yamaguchi, S. Uchida, Y. Nakagawa, K. Uehara and K. Kamata, *Catal. Today*, 2006, **117**, 32–36.
- 14 D. Hagrman, P. J. Hagrman and J. Zubieta, *Angew. Chem., Int. Ed.*, 1999, **38**, 3165.
- 15 C. Streb, C. Ritchie, D.-L. Long, P. K  gerler and L. Cronin, *Angew. Chem., Int. Ed.*, 2007, **46**, 7579.
- 16 C. Inman, J. M. Knaust and S. W. Keller, *Chem. Commun.*, 2002, 156–157.
- 17 H. Q. Tan, Y. G. Li, Z. M. Zhang, C. Qin, X. L. Wang, E. B. Wang and Z. M. Su, *J. Am. Chem. Soc.*, 2007, **129**, 10066.
- 18 C. Y. Sun, S. X. Liu, D. D. Liang, K. Z. Shao, Y. H. Ren and Z. M. Su, *J. Am. Chem. Soc.*, 2009, **131**, 1883.
- 19 S. T. Zheng, J. Zhang, X. X. Li, W. H. Fang and G. Y. Yang, *J. Am. Chem. Soc.*, 2010, **132**, 15102.
- 20 M. Dusi, T. Mallat and A. Baiker, *Catal. Rev.: Sci. Eng.*, 2000, **42**, 213–278.
- 21 H. C. Kolb, M. S. VanNieuwenhze and K. B. Sharpless, *Chem. Rev.*, 1994, **94**, 2483–2547.
- 22 E. M. McGarrigle and D. G. Gilheany, *Chem. Rev.*, 2005, **105**, 1563–1602.
- 23 J. Du, X. Y. Lai, N. L. Yang, J. Zhai, D. Kisailus, F. B. Su, D. Wang and L. Jiang, *ACS Nano*, 2010, **5**, 590–596.
- 24 J. L. Wang, X. D. Yang, K. Zhao, P. F. Xu, L. B. Zong, R. B. Yu, D. Wang, J. X. Deng, J. Chen and X. R. Xing, *J. Mater. Chem. A*, 2013, **1**, 9069–9074.
- 25 S. Wang, L. X. Yi, J. E. Halpert, X. Y. Lai, Y. Y. Liu, H. B. Cao, R. B. Yu, D. Wang and Y. L. Li, *Small*, 2012, **8**, 265–271.
- 26 N. L. Yang, Y. Y. Liu, H. Wen, Z. Y. Tang, H. J. Zhao, Y. L. Li and D. Wang, *ACS Nano*, 2013, **7**, 1504–1512.
- 27 H. J. Tang, H. J. Yin, J. Y. Wang, N. L. Yang, D. Wang and Z. Y. Tang, *Angew. Chem., Int. Ed.*, 2013, **52**, 5585–5589.
- 28 W. P. Griffith, *Transition Met. Chem.*, 1991, **16**, 548.
- 29 C. L. Hill and C. M. Prosser-McCartha, *Coord. Chem. Rev.*, 1995, **143**, 407.
- 30 R. Neumann, *Prog. Inorg. Chem.*, 1998, **47**, 317.
- 31 R. Ben-Daniel, L. Weiner and R. Neumann, *J. Am. Chem. Soc.*, 2002, **124**, 8788–8789.
- 32 N. Mizuno, K. Yamaguchi and K. Kamata, *Coord. Chem. Rev.*, 2005, **249**, 1944–1956.
- 33 C. L. Hill and R. B. Brown, *J. Am. Chem. Soc.*, 1986, **108**, 536–538.
- 34 R. Neumann and M. Gara, *J. Am. Chem. Soc.*, 1994, **116**, 5509–5510.
- 35 I. C. M. S. Santos, M. M. Q. Sim  es, M. M. M. S. Pereira, R. R. L. Martins, M. G. P. M. S. Neves, J. A. S. Cavaleiro and A. M. V. Cavaleiro, *J. Mol. Catal. A: Chem.*, 2003, **195**, 253.
- 36 S. Sakaguchi, Y. Nishiyama and Y. Ishii, *J. Org. Chem.*, 1996, **61**, 5307.
- 37 Z. W. Xi, N. Zhou, Y. Sun and K. L. Li, *Science*, 2001, **292**, 1139–1141.
- 38 P. Battioni, J. Renaud, J. Bartoli, M. Reina-Artiles, M. Fort and D. Mansuy, *J. Am. Chem. Soc.*, 1988, **110**, 8462–8470.
- 39 C. Venturello, E. Alneri and M. Ricci, *J. Org. Chem.*, 1983, **48**, 3831–3833.
- 40 B. S. Lane, M. Vogt, V. J. DeRose and K. Burgess, *J. Am. Chem. Soc.*, 2002, **124**, 11946–11954.
- 41 D. E. De Vos, J. L. Meinershagen and T. Bein, *Angew. Chem., Int. Ed.*, 1996, **35**, 2211–2213.
- 42 K. Mu    , J. Streuff, C. H. H  velmann and A. N    ez, *Angew. Chem., Int. Ed.*, 2007, **46**, 7125–7127.
- 43 R. B. Vamatta, C. C. Franklin and J. S. Valentine, *Inorg. Chem.*, 1984, **23**, 412.
- 44 J. F. Kinneary, J. S. Albert and C. J. Burrows, *J. Am. Chem. Soc.*, 1988, **110**, 6124.
- 45 V. Mirkhani, M. Moghadam, S. Tangestaninejad, I. Mohammadpoor-Baltork, E. Shams and N. Rasouli, *Appl. Catal., A*, 2008, **334**, 106–111.
- 46 I. D. Brown and D. Altermatt, *Acta Crystallogr., Sect. B: Struct. Sci.*, 1985, **41**, 244.
- 47 B. Keita, D. Bouaziz and L. Nadjo, *J. Electroanal. Chem.*, 1988, **255**, 307.
- 48 E. Itabashi, *Bull. Chem. Soc. Jpn.*, 1987, **60**, 1333.
- 49 B. Keita, A. Belhouari, L. Nadjo and R. Contant, *J. Electroanal. Chem.*, 1995, **381**, 243.
- 50 J. P. Launay, R. Massart and P. Souchay, *J. Less-Common Met.*, 1974, **36**, 79.
- 51 M. D. Hughes, Y.-J. Xu, P. Jenkins, P. McMorn, P. Landon, D. I. Enache, A. F. Carley, G. A. Attard, G. J. Hutchings and F. King, *Nature*, 2005, **437**, 1132–1135.
- 52 B. D. Li, P. He, G. Q. Yi, H. Q. Lin and Y. Z. Yuan, *Catal. Lett.*, 2009, **133**, 33–40.
- 53 L. L. Zhang, H. C. Zhang, W. S. Zhang, J. J. Gong, H. L. Hu, Y. N. Yang, Y. Liu and Z. H. Kang, *Dalton Trans.*, 2012, **41**, 13277–13279.
- 54 D. Farrusseng, S. Aguado and C. Pinel, *Angew. Chem., Int. Ed.*, 2009, **48**, 7502–7513.
- 55 A. Henschel, K. Gedrich, R. Kraehnert and S. Kaskel, *Chem. Commun.*, 2008, 4192–4194.
- 56 J. Lee, O. K. Farha, J. Roberts, K. A. Scheidt, S. T. Nguyen and J. T. Hupp, *Chem. Soc. Rev.*, 2009, **38**, 1450–1459.
- 57 K. Schlichte, T. Kratzke and S. Kaskel, *Microporous Mesoporous Mater.*, 2004, **73**, 81–88.

- 58 G. J. Zhang, H. Li, F. F. Zhao, H. L. Hu, H. Huang, H. T. Li, X. Han, R. H. Liu, H. Dong, Y. Liu and Z. H. Kang, *Dalton Trans.*, 2013, **42**, 9423–9427.
- 59 R. Neumann, *Inorg. Chem.*, 2010, **49**, 3594–3601.
- 60 R. Neumann and M. Dahan, *Nature*, 1997, **388**, 353–355.
- 61 R. Neumann and M. Dahan, *J. Am. Chem. Soc.*, 1998, **120**, 11969–11976.
- 62 C. H. A. Tsang, Y. Liu, Z. H. Kang, D. D. D. Ma, N.-B. Wong and S.-T. Lee, *Chem. Commun.*, 2009, 5829–5831.